Investigating the role of extracellular polymeric substances produced by *Parachlorella kessleri* in Zn(II) bioremediation using atomic force microscopy

Victoria Passucci[a, b], Ophélie Thomas-Chemin[c], Omar Dib[d], Antony Ali Assaf[d], Marie-José Durand[d], Etienne Dague[c], Maria Mar Areco[a, b*] and Cécile Formosa-Dague[e*]

[a] IIIA-UNSAM-CONICET, Instituto de Investigación e Ingeniería Ambiental, Escuela de Hábitat y Sostenibilidad (EHyS), Universidad Nacional de San Martín (UNSAM), Campus Miguelete, 25 de mayo y Francia, 1650-San Martín, Provincia de Buenos Aires, Argentina

[b] Consejo Nacional de Investigaciones Científicas y Técnicas (CONICET). Godoy Cruz 2290 CP (1033), Buenos Aires, Argentina.

[c] LAAS-CNRS, Université de Toulouse, CNRS, 31400 Toulouse, France

[d] Nantes Université, ONIRIS, CNRS, GEPEA, UMR 6144, La Roche-sur-Yon, F-85000, France

[e] TBI, Université de Toulouse, INSA, INRAE, CNRS, 31400 Toulouse, France

Corresponding authors: Maria M. Areco, mareco@unsam.edu.ar
Cécile Formosa-Dague, formosa@insa-toulouse.fr

Abstract

Microalgae, such as *Parachlorella kessleri*, have significant potential for environmental remediation, especially in removing heavy metals like zinc from water. This study investigates how *P. kessleri*, isolated from a polluted river in Argentina, can remediate zinc. Using atomic force microscopy (AFM), the research examined the interactions between Zn particles and cells grown with different nitrogen sources—nitrate or ammonium. The results showed that cells grown with nitrate produced extracellular polymeric substances (EPS), while those grown with ammonium did not. Raman spectroscopy revealed distinct metabolic responses based on the nitrogen source, with nitrate-grown cells showing altered profiles after zinc exposure. Zinc exposure also changed the surface roughness and nanomechanical properties of the cells, particularly in those producing EPS. AFM force spectroscopy experiments then confirmed strong Zn binding to EPS in nitrate-grown cells, while interactions were weaker in ammonium-grown cells that lacked EPS. Overall, our results elucidate the critical role of EPS in Zn removal by *P. kessleri* cells and show that Zn remediation by *P. kessleri* is mediated by EPS adsorption. This study underscores the significance of regulating nitrogen sources to stimulate EPS production, offering insights that are essential for subsequent bioremediation applications.

Keywords

Parachlorella kessleri, bioremediation, heavy metal, extracellular polymeric substances, atomic force microscopy

1. Introduction

Rivers are the main source of clean water in many parts of the world. Their contamination represents a problem not only for the populations living nearby, but also for the ecosystems linked to the streams. The Reconquista River, located in the province of Buenos Aires, Argentina, is an example of a heavily polluted river, as it receives tributaries from both domestic and industrial sources with varying levels of contamination. Nutrients, such as nitrate and ammonium, and heavy metals are among the pollutants found in the water and sediments (Basílico et al., 2022; Tufo et al., 2018). Contamination levels vary between the upper, middle, and lower basins, and different biological community compositions can be found along the river. In particular, microalgae are found in water and sediment, even in the middle and lower Reconquista basins where contamination levels are higher due to the discharge of industrial and domestic effluents. These microalgae are adapted to live in extreme conditions, making them suitable for a variety of biotechnological applications (Castañé et al., 1998; Ferraro et al., 2021; Grimolizzi, 2019).

Microalgae are highly diverse phototrophic organisms that play an important role in the global carbon and nutrient cycles. They also have the capacity to produce commercially viable metabolites for pharmaceutical, nutraceutical and industrial applications (Sreenikethanam et al., 2022). Among their many interests, in recent years, they have attracted attention for their remediation potential (Areco et al., 2021; Dayana Priyadharshini et al., 2021; Rude et al., 2022; Li and Meng, 2023). Indeed, their presence in an aquatic environment can reduce high concentrations of phosphate, nitrate and ammonium that generally cause eutrophication in rivers and lakes (Kakade et al., 2021). Also, many studies demonstrate that some microalgae can interact with heavy metals and reduce their concentrations in solution (Areco et al., 2018, 2022; Spain et al., 2021). Other studies highlight the benefits of this bioremediation approach, noting that it can generate biomass for producing commercially valuable byproducts as part of a biorefinery strategy (Satya et al., 2023; Tripathi et al., 2023). It has been found that the main mechanisms involved in heavy metal remediation by microalgae are metal precipitation due to pH changes linked to their nitrogen metabolism (Areco et al., 2022) and passive adsorption, or biosorption, owing to their large surface area and high binding affinity, which varies among species.

Biosorption is a surface phenomenon that occurs independently of microbial metabolism. The size, shape, and cell wall composition of different algal species can affect their metal binding capabilities. The process mainly involves the interaction between positively charged metal ions and negatively charged cell surfaces (Gupta and Diwan, 2017). Even though many papers describe heavy metal biosorption process (He and Chen, 2014; Volesky, 2007), for the moment, the molecular basis of the interactions between the microalgae cell surface and heavy metals, and therefore the mechanisms underlying their adsorption, are not entirely clear. For instance, an important question that still requires clarification is the role played by extracellular polymeric substances (EPS) attached to the cells in the adsorption of the heavy metals. EPS are a diverse group of macromolecules that are secreted in relative high amounts by several genera of eukaryotic red and green microalgae, such as *Parachlorella kessleri*, and some prokaryotic microalgae (Xiao and Zheng, 2016; Sendra et al., 2017). Different factors, such as culture conditions, can potentially influence the generation and structure of EPS, even those derived from the same species (Sasaki et al., 2020; Ye et al., 2022). They can include polysaccharides, proteins, lipids, and nucleic acids, and can vary in composition and structure depending on the microalgae species (Wang et al., 2018). EPS may provide many beneficial

functions for the microalgae, including energy storage, cell-to-cell communication, and protection from environment stressors, among others. In addition, EPS can also play a role in shaping the microalgae environment, by contributing to the formation of biofilms and aggregates and by mediating the interaction with other organisms and/or abiotic components, such as dissolved pollutants (Ciempiel et al., 2022). In this sense, they could also play a key role in the interaction with heavy metals and in the further bioremediation capacities of cells, given that EPS have demonstrated a remarkable affinity for heavy metals (Li et al., 2022).

Using microalgae adapted to leave in polluted environments is crucial when studying the possibility to apply bioremediation to contaminated waters (Afonso et al., 2024). In this sense, several species have been isolated from the Reconquista River in order to study their remediation potential. Among them is *Parachlorella kessleri*, a green microalgae species that generates EPS. *P. kessleri* has been studied for its potential to grow with different nitrogen sources (O'Rourke et al., 2015; Lv et al., 2019). Notably, in these studies, it was showed that depending on the nitrogen source, nitrate or ammonium, the capacity of *P. kessleri* cells to remove pollutants from water was different and was better when cells were in the presence of nitrate. Another study showed that *P. kessleri* cells were able to remove heavy metals from water, in particular cadmium and chromium, and could thus be considered as a bioremediation agent for this type of pollutants (Bauenova et al., 2021). Furthermore, our team has obtained preliminary results indicating that the remediation of Zn(II) by *P. kessleri* varies when cultivated in different nitrogen sources. Thus, in this study, we chose to evaluate the interactions of Zn(II) and *P. kessleri* when cultivated in different nitrogen sources, ammonium and nitrate. Our aim is to understand cell-Zn interactions when microalgae are cultured with different nitrogen sources and elucidate the potential role of the EPS they produce in the remediation. To conduct such study, we chose to work with atomic force microscopy (AFM) as a main tool. Since its initial development in 1986 (Binnig et al., 1986), AFM has emerged as a powerful tool for nanoscale surface characterization. Beyond its capabilities for high-resolution imaging down to the nanometer scale, AFM is also a sensitive force machine capable of capturing forces at the piconewton level (Dufrêne et al., 2017). This characteristic enables the exploration of nanomechanical and adhesive properties of samples, as well as their interactions with their environment. In the specific field of microalgae studies, AFM has been instrumental in unraveling the morphology, nanostructure, nanomechanics, and adhesive behavior of cells (Formosa-Dague et al., 2018; Demir-Yilmaz et al., 2021, 2023c). Notably, it has provided insights into their interactions with particles or molecules present in their environment (Demir et al., 2020; Demir-Yilmaz et al., 2022) and on the properties of the EPS they can produce (Vergnes et al., 2019).

In this work, we will first evaluate the effect of different nitrogen sources, ammonium and nitrate, as well as Zn(II) on the metabolism of *P. kessleri* by determining the spectral fingerprints of the cell metabolites, such as chlorophyll a, beta-carotene, nucleic acids and lipids, through Raman spectroscopy. Then AFM will be used to understand the effect of the nitrogen source on the EPS production, to evaluate the effects of the presence of Zn(II) on the cells and their EPS, and finally to probe the interactions between Zn particles and cells at the molecular scale. This approach will enable to assess the possibility of using *P. kessleri* cells to decontaminate heavy metals from water, by providing a complete understanding of the mechanisms involved in the interactions between cells and the Zn(II) present in the medium. Such findings could have great impacts on environmental management and to develop efficient bioremediation strategies.

2. Experimental Section

2.1. Microalgae strain and culture

P. kessleri was obtained from the culture collection of the Environmental Research and Engineering Institute (IIIA CONICET-UNSAM). This strain was previously isolated from the sediments of the middle basin of the Reconquista River, at San Francisco Park (S 34°34'14.8" W 58°39'46.4"). Cells were cultivated in sterile conditions in two different nutritive condition. The culture medium used was Bold Basal Medium (BBM) containing either $NaNO_3$ (BBM-NO_3^-, nitrate condition) or $(NH_4)_2SO_4$ (BBM-NH_4^+, ammonium condition) as a nitrogen source, with the same initial nitrogen concentration (≈ 2.9 mM). Initial pH comprised between 6 and 6.5. The cultures were maintained at 21°C, under 120 rpm of orbital agitation, in an incubator (Panasonic, Japan) equipped with white neon light tubes providing an illumination of approximately 40 µmol photons m^{-2} s^{-1}, with a photoperiod of 18 h light: 6h dark. All experiments were performed with 7 days exponential phase batch cultures. For cultures in the presence of Zn(II), the same procedure was conducted, but an aliquot of a concentrated solution of $ZnSO_4 \cdot 7H_2O$ (30 mM of Zn(II)) was added to each culture (BBM-NO_3^- and BBM-NH_4^+), resulting in a final concentration of 0.25 mM of Zn(II). The initial pH was adjusted to 5.5 to avoid metal precipitation.

2.2. Cellular metabolites characterization using RAMAN spectrometry

The Raman spectra were obtained from freeze-dried pellets of *P. kessleri* using a Raman microspectrometer Bruker Optics, (Senterra, Germany) driven by Opus software (Bruker Optics, v7.2). This device was equipped with a CCD camera cooled at - 60°C and a BX51 Olympus microscope. Spectral data were collected using a 532 nm excitation laser with a power output of 2mW at the sample. Each spectrum was obtained by averaging five sequential acquisitions, each with an integration time of 10 seconds (Lieutaud et al., 2019). Raman spectra were processed using MATLAB software (version R2019b, MathWorks Inc, Natick, MA, USA). The raw data, covering a spectral range of 170–4000 cm^{-1}, was first cut in the spectral zone of 170–1600 cm^{-1}. All spectra were subsequently baseline corrected employing an elastic concave method (64° and ten iterations), smoothed using the Savitzky-Golay algorithm, and finally normalized via min–max normalization. The treated spectra were subjected to multivariate data analysis, specifically Principal Component Analysis (PCA). The optimal number of principal components (PCs) was determined using a scree plot. Then, PC scores (specifically PC1 scores) were subjected to the Kruskal Wallis (KW) test, a non-parametric method for comparing samples from three or more groups of independent observations (Kruskal and Wallis, 1952). Both PCA and KW were computed using the SAISIR Package (Cordella and Bertrand, 2014). All statistical analysis was performed using MATLAB software (version R2019b, MathWorks Inc., Natick, MA, USA).

2.3. Cell immobilization for AFM experiments

Before AFM experiments, 1 mL of cells from 7-days cultures were diluted into 5 mL of either BBM-NO_3^- or BBM-NH_4^+. After that, cells were immobilized on polyoctyl-chitosan (PO-chitosan) coated glass slides. For that, briefly, a 1.0 g L^{-1} solution of PO-chitosan synthesized in a previous study was spin-coated on plasma cleaned glass surfaces at 1000 rpm for 3 min (Demir-Yilmaz et al., 2023a). The glass slides were then dried in an incubator at 37°C overnight before use. Then, 1 mL of cell suspension was deposited on the surface, incubated during 30 min, and rinsed using either BBM-NO_3^- or BBM-NH_4^+ before performing the AFM experiments.

2.4. AFM imaging and roughness analysis

Height images of the whole cells were recorded using the Quantitative Imaging mode available on the Nanowizard IV XP AFM (Bruker, USA), with MLCT cantilevers (Bruker, nominal spring constant of 0.01 N m^{-1}). Images were recorded with a resolution of 150 × 150 pixels using an applied force comprised between 0.8 and 1.5 nN and a z-length comprised between 1 and 6 µm. In all cases, the cantilevers spring constants were determined using the thermal noise method prior to imaging (Hutter and Bechhoefer, 1993). To obtain high-resolution height images of the cell surface for roughness analysis, small areas of 0.5 × 0.5 µm on top of cells were recorded using the contact mode available on the Nanowizard IV XP AFM (Bruker, USA), with MLCT cantilevers (Bruker, nominal spring constant of 0.01 N/m), at a resolution of 512 lines, using an applied force < 1 nN. The height images obtained were then analyzed using the data processing software (Bruker, USA) to determine the arithmetic average roughness (Ra). In each condition, 10 different images were recorded on 10 different cells coming from at least two independent cultures. To assess the significance of the differences observed between the different conditions tested, non-parametric statistical Mann and Whitney test was used. The differences were considered significant at p-value < 0.05.

2.5. AFM nanomechanical analysis

For nanoindentation experiments, the AFM was used in force spectroscopy mode using an applied force comprised between 0.5 and 5 nN depending on the condition, with MLCT cantilevers (Bruker, nominal spring constant of 0.01 N m^{-1}). Young's moduli were then calculated from 70 nm indentation curves in the case of cells grown in BBM-NH_4^+, and 500 nm indentation curves in the case of cells grown in BBM-NO_3^- using the Hertz model (Hertz, 1881) in which the force F, indentation (δ), and Young's modulus (Ym) follow Equation 1, where α is the tip opening angle (17.5°), and υ the Poisson ratio (arbitrarily assumed to be 0.5). The cantilevers spring constants were determined by the thermal noise method (Hutter and Bechhoefer, 1993):

$$F = \frac{2 \times Ym \times \tan\alpha}{\pi \times (1-\upsilon^2) \times \delta^2} \qquad (1)$$

In each condition, 10 different cells coming from at least 2 independent cultures were probed. To assess the significance of the differences observed between the different conditions tested, parametric statistical student t-test was used. The differences were considered significant at p-value < 0.05.

2.6. AFM dynamic mechanical analysis (DMA)

For these experiments, colloidal probes were used. These were prepared as previously described in (Beaussart et al., 2014). In brief, a single silica microsphere (5 µm of diameter, Bangs Laboratories) was attached to triangular tipless NP-O10 cantilevers (Bruker, USA) using a thin layer of UV-curable glue (NOA 63, Norland Edmund Optics). Then, measurements were performed by applying a determined force of 1 nN (initial indentation), before applying sinusoidal excitation signals at frequencies of 1, 10, 20, 50 and 100 Hz. During these measurement, in-phase and out-phase signals are detected, and further used to determine the shear modulus G^* using the following Equation 2, where G' is the storage modulus, G'' is the loss modulus, i is the complex unit, υ the Poisson ratio (assumed to be 0.5), δ_0 the initial indentation, R the spherical colloidal probe radius (here of 2.5 µm), δ^* the sinusoidal indentation, and F^* the sinusoidal force.

$$G^* = G' + iG'' = \frac{1-\upsilon}{4\sqrt{R\delta_0}} \frac{F^*}{\delta^*} \qquad (2)$$

From these measurements, the G' and G'' values were extracted from 70 curves recorded on 23 cells for each condition, and tan (δ) was calculated, which corresponds to the ratio of G'' over G'.

2.7. AFM cantilevers functionalization with Zn particles and force spectroscopy experiments

To prepare functionalized AFM cantilevers with Zn particles, the edge of NP-O10 tipless cantilevers (Bruker, USA) was first dipped into a thin layer of UV-curable glue (NOA63, Norland Edmund Optics). Then the cantilever was approached towards a metallic Zn particle deposited on a glass surface to attach it at the edge of it. The functionalized cantilevers were then put under UV-light for 10 min to allow the glue to cure. These functionalized cantilevers were used in force spectroscopy experiments to probe the interactions with cells grown either in BBM-NO_3^- or in BBM-NH_4^+ for 7 days. The interactions were recorded with an applied force of 0.25 nN, at a speed of 1 µm s^{-1}, using a contact time of 1 s. In each condition, 10 different cells coming from at least 2 independent cultures were probed using 5 different probes. To assess the significance of the differences observed between the different conditions tested, parametric statistical student t-test was used. The differences were considered significant at p-value < 0.05.

2.8. Scanning electron microscopy imaging of AFM cantilevers

AFM cantilevers with tips functionalized or not were imaged using a Jeol 6400 electron microscope (Jeol,Tokyo, Japan) equipped with an EDS Bruker SDD detector, at an acceleration voltage of 20 kV.

3. Results and Discussion

3.1. The nitrogen source influences the production of EPS by cells

It is well known that nutritive conditions can affect the production of EPS by microalgae cells. This has already been showed for different microalgae species (Wang et al., 2014; Babiak and Krzemińska, 2021), and in the case of *P. kessleri*, one study has showed that a deprivation in nitrogen could lead to an overproduction of EPS by the cells (Sasaki et al., 2020). In addition, a study performed in 1994 showed that in the case of *Botryococcus braunii,* the amount of EPS produced was different depending on the nitrogen source. In particular, it was showed that the highest production of EPS was detected in the presence of nitrate and that the lowest yield was obtained in the presence of ammonium (Lupi et al., 1994). To verify if this was also the case for the *P. kessleri* cells used in this study, we first used AFM to image cells and detect the presence of EPS in the two different nutritive conditions. The results obtained are presented in Fig. 1. In the case of cells grown in the presence of nitrate (Fig. 1A), cells present a spherical shape, but the edges of the cells are not well-resolved, indicating that the tip could not get into contact with them during the acquisition. Moreover, as indicated by the arrow on Fig. 1A, some material seems to surround the cell. This is confirmed by the cross-section taken along the white dashed line (Fig. 1C) that shows that indeed, the cell is surrounded by a layer of approximately 1 µm in height, that could correspond to EPS. When cells are grown with ammonium (Fig. 1B), the AFM image obtained shows also a spherical cell but this time, the edges are well-resolved, which tends to indicate that no layer of material could prevent the tip to get into direct contact with the cell. This is also confirmed by the cross-section (Fig. 1D) that shows that no material surrounds the cell. Thus, these imaging results indicate that cells grown with nitrate produce a layer of material, most likely EPS, that is not detected when they grow with ammonium. This was further confirmed by SEM imaging experiments, (Fig. S1) which also demonstrated that EPS are present in a greater extent when cells are grown with nitrate than when they are grown with ammonium. It is important to note that the EPS observed on ammonium-grown cells in SEM images might be soluble EPS, made visible due to the sample preparation process. These EPS most likely are not bound to the cell surface, explaining why they are not detected under the physiological conditions in which the AFM experiments were conducted.

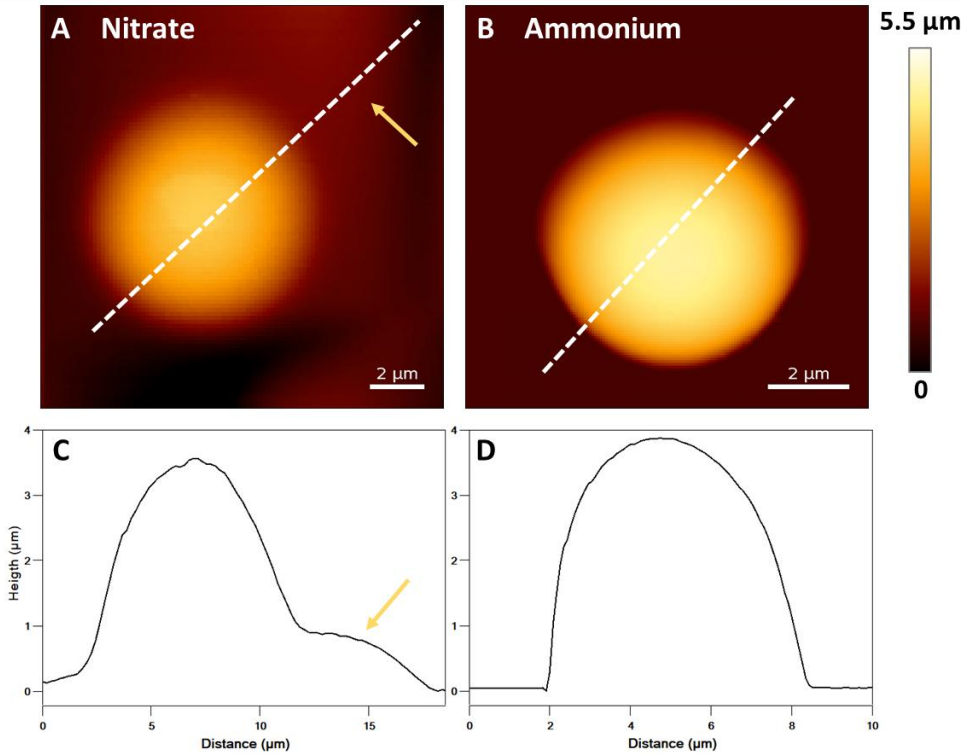

Fig. 1. AFM imaging of P. kessleri in different nutritive conditions. *A) AFM height image of a P. kessleri cell grown with nitrate and B) grown with ammonium. The yellow arrow in A) indicates the presence of a layer of material surrounding the cell. C) and D) Cross-section taken along the white dashed line in A) and B) respectively. The yellow arrow in C) corresponds to the layer of material observed in A).*

We then further characterized the EPS layer surrounding the cells by performing two different types of experiments: roughness measurements and nano-indentations experiments. First, to perform roughness measurements, images of small areas of 0.5 x 0.5 µm were recorded on top of the cells using AFM in contact mode. This recording mode enables the acquisition of images with nanoscale resolution, offering the capability to unveil the ultrastructure of the cell surface. The images obtained for both cells grown with nitrate or with ammonium are showed in Fig. 2A and B. They both show a rather rough surface, featuring structures which are several nm in height, as indicated by the cross-section taken along the white lines in both images (Fig. 2C and D). Quantitative analysis was then performed using images recorded on 10 different cells in each condition to determine the average roughness, which is of 1.9 ± 0.3 nm for cells grown with nitrate, and of 1.9 ± 0.7 nm for cells grown with ammonium (Fig. 2E). Cells in both conditions thus exhibit a similar surface structure, which is surprising. Indeed, in the case of cells grown with nitrate, the cells are covered by an EPS layer, and this is the EPS layer that should be imaged. While for cells grown in the presence of ammonium, there is no EPS layer on top of cells thus the images show directly the cell surface. There are two options; either both the EPS and the cell surface have a similar ultrastructure, or one possibility is that the EPS layer on top of cells is too soft, so that the tip goes through it directly and touches the cell surface. While EPS of microalgae cells have been imaged using AFM when deposited on surfaces (Cybulska et al., 2016) or in dried conditions (Demir-Yilmaz et al., 2023b), no images of EPS imaged directly on top of cells in liquid conditions have been reported. However, one previous AFM study conducted in our team showed that EPS produced by a cyanobacteria formed a gel-like material that was extremely soft (approximately 20 kPa). If this is also the case for *P. kessleri* cells, it could elucidate why the force applied by the tip in contact imaging, even when kept at a low level,

might be enough to penetrate the EPS layer. To verify this point, we then performed nano-indentation experiments to determine the nanomechanical properties of cells grown in both nutritive conditions. In this type of experiment, the tip, with known mechanical properties, is pressed against the surface at a known applied force and retracted. This gives access to nano-indentation curves, that can then be fitted by a model to extract the Young modulus (Ym) value, that corresponds to the rigidity of the cell surface, *i.e.* its resistance to compression. The lower the Ym value, the softer the material. The results obtained by probing 10 different cells in each condition show an important difference between the two nutritive conditions. Indeed, cells cultured with nitrate exhibit a remarkably low average Young's modulus (Ym) value of 0.4 ± 0.1 kPa. In contrast, for cells cultivated with ammonium, the average Ym value is higher at 880.1 ± 727.4 kPa (Fig. 2F). The value recorded for ammonium cells is in line with measurements performed on the cell wall of other microalgae species (Demir et al., 2020; Demir-Yilmaz et al., 2023c), and reflects the rigidity of the cell wall. However, the value obtained for cells grown with nitrate is very low, and most likely corresponds to the nanomechanical properties of the EPS present on top of the cells, that form, like it was previously showed, a gel-like structure (Vergnes et al., 2019). Given this, it is then most likely that the contact image recorded (Fig. 2A) corresponds to the cell wall and not to the EPS layer. Thus, it can be concluded that the different nitrogen source does not have an effect on the cell wall ultrastructure, even though the metabolism of cells may be different in these two conditions.

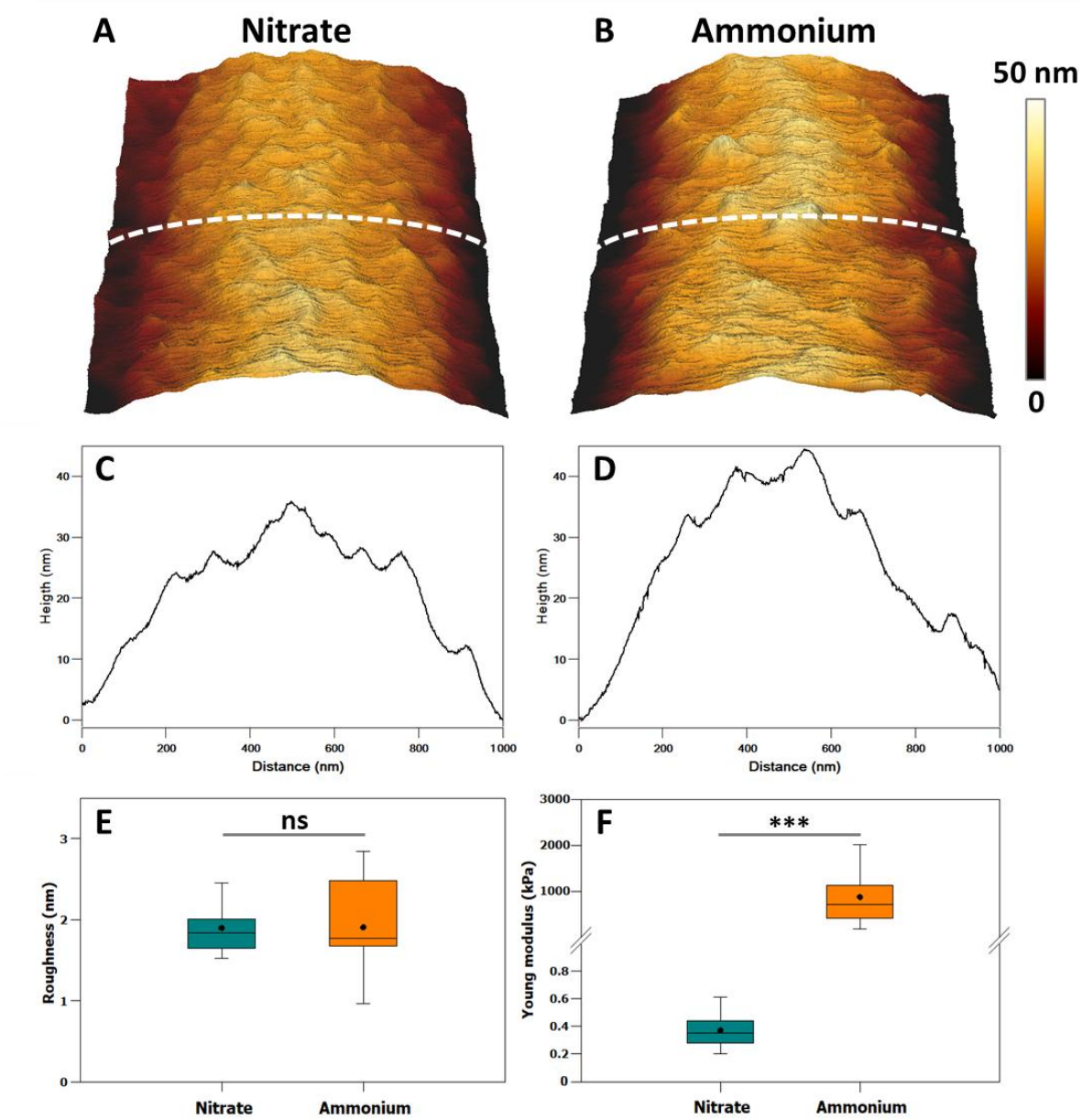

Fig. 2. AFM characterization of P. kessleri cell surface. *A) AFM height image of an area of 0.5 x 0.5 µm on top of a cell grown in the presence of nitrate or B) in the presence of ammonium. C) and D) Cross-sections taken along the white dashed lines in A) and B) respectively. E) Boxplot showing the distribution of roughness values obtained on 10 different cells coming from at least two independent cultures for both nutritive conditions. F) Boxplot showing the distribution of Ym values recorded on 10 different cells coming from at least two independent cultures for both nutritive conditions.*

3.2. Exposure of cells to Zn affects their surface properties

In a next step, we then repeated these experiments with cells exposed during culture to a Zn(II) concentration of 0.25 mM in both nutritive conditions. The first aspect was to check if the exposure to Zn could have an impact on the EPS production, as in some cases, it has been showed that the exposure of cells to a stress could result in the overproduction of EPS by the cells (Pletikapić et al., 2012). For that, AFM images of the whole cells were recorded, and showed no differences with the ones obtained with cells that had not been exposed to Zn(II) (Fig. S2). Thus it does not seem that Zn(II) exposure has an effect on the EPS production. We then took a closer look at the surface of cells

and measured their roughness and nanomechanical properties. The results obtained are presented in Fig. 3. The ultrastructure observed for cells without Zn(II) (Fig. 2A and B) seems to be conserved only in the case of cells grown with ammonium. Indeed, cells grown with nitrate present a smooth surface in the presence of Zn(II) with no structures emerging from the surface as indicated by the cross-section in Fig. 3C. For cells grown with ammonium, the cross-section indicate the presence of structures at the surface of cells that seem to have a height increased compared to the condition without Zn(II). To confirm these observations, the quantitative analysis on the images recorded showed that the average roughness in the case of cells grown with nitrate is of 0.5 ± 0.3 nm, and of 2.8 ± 0.5 nm for cells grown with ammonium (Fig. 3E). Thus, the response of the cells to the presence of the pollutant in the culture medium is different depending on the nitrogen source used. For cells grown with nitrate, the cell wall becomes smooth, while for cells grown with ammonium, it becomes rougher, featuring higher structures on its surface. Regarding the nanomechanical properties, there are also important changes compared to the conditions without Zn(II). For instance, for cells grown with nitrate, the average Ym value decreases from 0.4 ± 0.1 kPa to 0.2 ± 0.1 kPa with Zn(II) and for cells grown with ammonium, it decreases from 880.1 ± 727.4 kPa to 478.3 ± 225.1 kPa in the presence of Zn(II) (the differences in both cases are significant at a p-value of 0.001, student t-test).

A few AFM studies of the microalgae cell surface changes induced by an exposure to heavy metal pollutant are available in the literature. In one of this study, the effects of cadmium were evaluated on a green microalgae species, *Dunaliella tertiolecta* (Ivošević DeNardis et al., 2019). Their results showed that cells in the presence of cadmium had a cell wall 80% more rigid compared to control cells. While our results are opposite in the sense that cells get softer in the presence of Zn(II), they are still in line with the fact that heavy metal exposure has an impact on the cell's nanomechanical properties. Moreover other stress conditions have been studied using AFM, such as salinity changes (Demir-Yilmaz et al., 2023b), N-deprivation (Yap et al., 2016), or pH changes (Formosa-Dague et al., 2018; Pillet et al., 2019). All these different stresses resulted in changes in the nanomechanical properties of cells. These alterations are frequently linked to modifications either in the biochemical composition of the cell wall, which can shift as cells adjust their metabolism in response to stress, or to a restructuring of the cell wall architecture. This restructuring implies that the various components of the cell wall can be reorganized to adapt to the stress (Demir-Yilmaz et al., 2023c). Regarding cell surface roughness, this parameter has also been showed to be impacted by stress condition in microalgae. For instance, in the case of *C. vulgaris*, our team has previously showed that both a salinity change in the culture medium or a change in the pH had for consequence to increase the cell wall roughness (Demir et al., 2020; Demir-Yilmaz et al., 2023c). In these investigations, it was proposed that this might be attributed to a rearrangement of molecules at the cell surface, protruding more prominently under stress conditions, consequently causing the observed increased roughness.

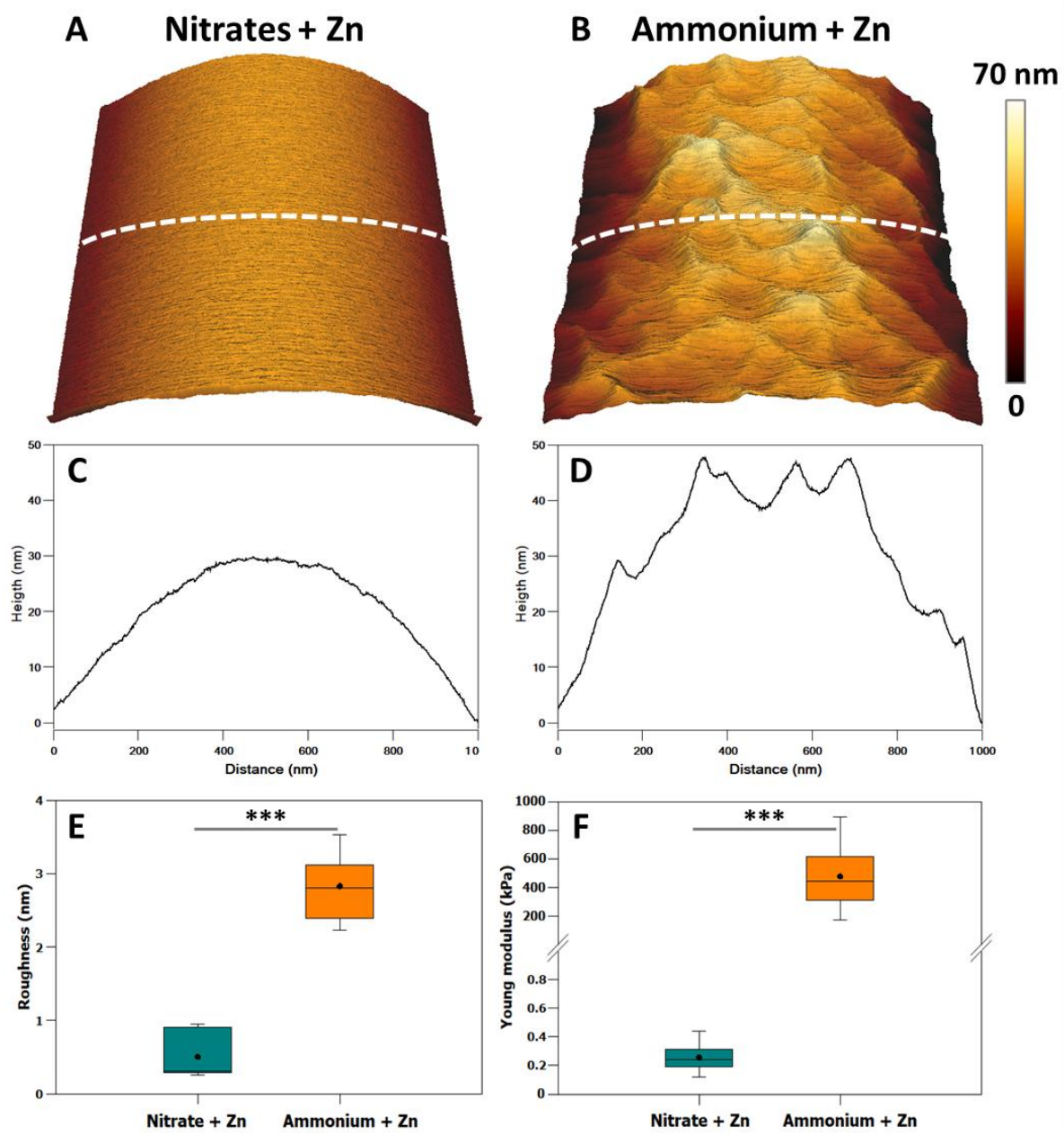

Fig. 3. AFM characterization of P. kessleri cell surface upon exposure to Zn(II). *A) AFM height image of an area of 0.5 x 0.5 µm on top of a cell grown in the presence of nitrate and Zn(II) at a concentration of 0.25 mM or B) in the presence of ammonium and Zn(II) at a concentration of 0.25 mM. C) and D) Cross-sections taken along the white dashed lines in A) and B) respectively. E) Boxplot showing the distribution of roughness values obtained on 10 different cells coming from at least two independent cultures for both nutritive conditions in the presence of Zn(II). F) Boxplot showing the distribution of Ym values recorded on 10 different cells coming from at least two independent cultures for both nutritive conditions in the presence of Zn(II).*

3.3. The metabolism of P. kessleri is affected both by the nitrogen source and the exposure to Zn(II)

In a next step, Raman spectroscopy was employed to investigate the impact of different culture media and Zn(II) exposure on the metabolism of *P. kessleri* cells. The Raman spectrum, detailed in the supplementary data (Fig. S3), highlights key peaks or molecule of interest detected

within the cells when they are exposed to the Raman laser. Microalgae, in general, exhibit common bands or Raman shifts at 957 δ(C-H_3), 1182 δ(C-H_3), 997 ν(C-C), 1149 ν(C-C), 1182 and 1571 ν(C-C) cm^{-1}, which are associated with chlorophylls and carotenoids. Additionally, a shift at 1436 cm^{-1} σ (C-H_2) indicates the presence of lipids (Wieser et al., 2023). To assess the effect of the different nitrogen sources (nitrate and ammonium) and of Zn(II) exposure on *P. kessleri* cells, a PCA multivariate statistical analysis was applied to the Raman spectra obtained in the different conditions. Fig. 4A shows that the first principal component PC1 accounts for the majority of spectral variances, explaining about 96.6 % of the variance, while the second principal component PC2 explains only 1.7%. All other principal components contained less than 1% of the variance between samples. The PCA plot demonstrates a clear separation between cells cultured with ammonium, indicated by negative score values on PC1, and those cultured with nitrate, indicated by positive sign on PC1. It seems that all bands with a negative sign on loading 1 (Fig.4B) are associated with cells cultured in ammonium as they have a negative sign on PC1 scores. This indicates that *P. kessleri* cells grown in culture medium with ammonium are strongly associated with higher level of chlorophyll, carotenoids and lipids as indicated by the negative loadings on PC1. In contrast, cells cultured with nitrate did not show the same high level of association with these biomolecules. This is further confirmed by the Kruskal Wallis test performed on PC1 scores, which shows that cells cultured with ammonium are significantly different ($p<0.05$) from those grown in nitrate (Fig 4D). These results thus show that the nitrogen source has an impact on the metabolism of cells, ammonium inducing the production in cells of more pigments (chlorophyll and carotenoids) and more lipids compared to nitrate. While Raman spectroscopy has already been used to evaluate the impact of nitrogen concentration in the culture medium (Zhang et al., 2017; He et al., 2018; Li et al., 2019), this is the first time that the impact of a different nitrogen source is evaluated. What is interesting to note is that in both cases, pigments and lipid contents were affected either by a changing nitrogen concentration, or in our case by a different nitrogen source. Our results are thus in line with existing literature on this topic.

Regarding the effect of adding Zn(II) to both cultures conditions, cells cultured with ammonium did not exhibit any significant changes as confirmed by PC1 results and Kruskal Wallis (no significant difference, $p > 0.05$). However, for cells cultured with nitrate as the nitrogen source, the addition of Zn(II) had a negative impact. This is indicated by loading 2 (Fig 4C), where carotenoids were more associated with cells cultured with nitrate and without Zn(II). The Kruskal Wallis test also indicated a significant difference between the latter two groups (Fig 4D). It is interesting to compare and correlate these results with the ones obtained using AFM. Indeed, in the case of cells grown with nitrate, AFM experiments showed that both the roughness and the mechanical properties of the EPS layer around the cells were impacted by the exposure to Zn(II). The Raman results obtained here show that these changes on the "outside" of the cell, are also associated with changes in the cell's metabolism as they present a lower level of carotenoids than cells that were not exposed to Zn(II). For cells grown with ammonium, while the cell's surface is also modified by the presence of Zn(II) in the medium (roughness and mechanical properties changed), cells do not have a modified metabolism. These observations suggest the following hypothesis: although both types of cells are in contact with the Zn(II) present in the culture medium, as indicated by the surface changes, only the cells grown with nitrate, which produce EPS, are affected by Zn(II), generating stress, as evidenced by metabolic changes observed here with Raman spectroscopy. The production of EPS by microalgae can have varying effects on the absorption of metals like Zn(II), that can be influenced by the microalgal species, environmental conditions, and the properties of the EPS. Indeed, EPS can either

hinder metal absorption by creating a protective layer around the cells, thus limiting direct metal uptake, or promote metal adsorption by forming complexes with the metal ions, which enhances the microalgae's ability to absorb these ions from the environment (Babiak and Krzemińska, 2021; Tripathi and Poluri, 2021). Furthermore, the solubility of EPS-metal complexes can influence the bioavailability of metals to microalgae (Hasani Zadeh et al., 2023). The results here obtained would suggest that EPS favors the absorption of the Zn present in the medium. To confirm this hypothesis, further investigation into the interactions between Zn(II) and the cells is necessary. Specifically, it should be verified whether the interaction of Zn(II) with the EPS produced by cells grown with nitrate

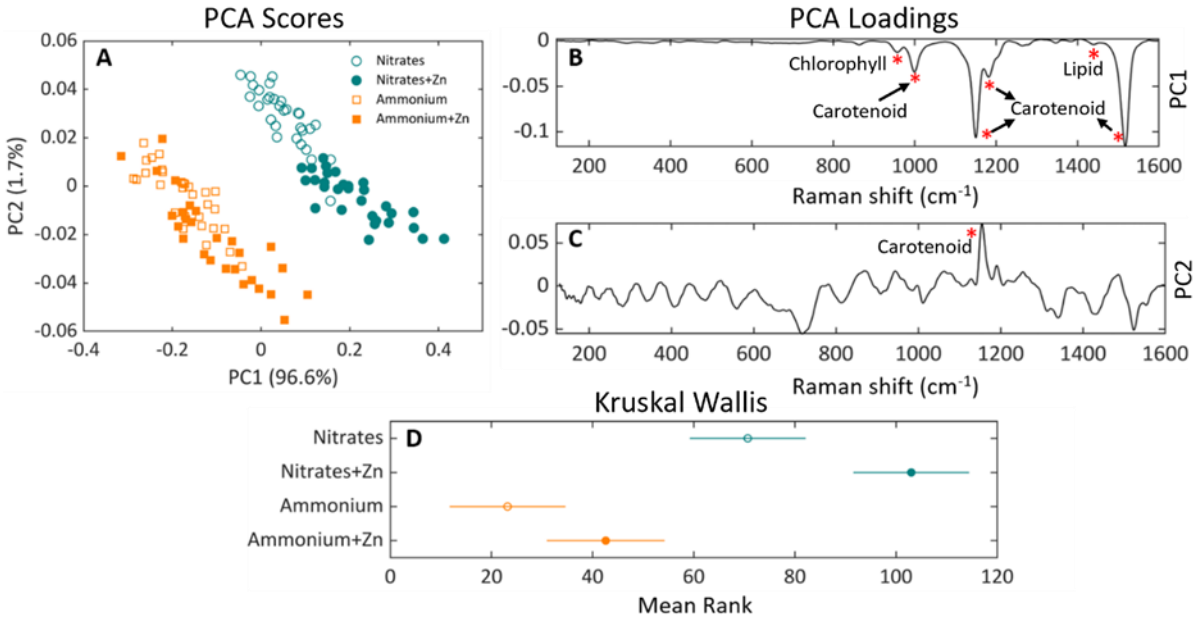

is indeed favored, thereby confirming the role of EPS in Zn(II) absorption into cells.

Fig. 4. PCA analysis of Raman spectra from Parachlorella kessleri cultivated using BBM with different nitrogenous compounds*. (A) The PC1 scores of P. kessleri cultivated with ammonium or ammonium + Zn are clearly distinguished from the two other groups. (B) The loading plot highlights the impacted molecules (represented by red asterisks) responsible for differentiating P. kessleri cultivated with ammonium or ammonium + Zn from the other groups on PC1. (C) The loading plot highlights the impacted molecules responsible for differentiating P. kessleri cultivated with nitrates from those cultivated with nitrates + Zn based on PC2. (D) Kruskal-Wallis on PC1 scores identify the groups that are significantly different from each other (p < 0.05).*

3.4. The EPS produced by cells interact and absorb zinc

To investigate the potential role of EPS in the interactions with Zn, we then conducted force spectroscopy experiments to probe the direct interactions between metallic Zn particles functionalized on cantilevers, and the surface of cells grown in both nutritive conditions. To functionalize the cantilever, a protocol that was previously developed in our team was used (Formosa-Dague et al., 2018), which allowed to produce cantilevers with a single particle attached at the edge of it, as it can been seen on the SEM images presented in Fig. S4. While AFM has already been used to characterize the effects of pollutants on microalgae cells, this is the first time the direct interactions between a pollutant and the surface of cells are probed. The results of the force spectroscopy experiments obtained are presented in Fig. 5. In these experiments, the functionalized cantilever is first approached towards the surface of the cells, stays in contact with it during 1 s, and is then retracted. This gives access to force curves, an example of which is presented in Fig. 5A. From

these force curves, a number of information on the interactions measured can be extracted. First, if an interaction takes place between the cantilever and the cell surface, the curves will present retract adhesions, that are materialized by negative peaks on the curve. By measuring the maximum height of these retract adhesions, it is possible to access to the adhesion force, *i.e.* the maximum force that was needed to break the interaction upon retraction (in yellow in Fig. 5A). Then, the area under the curve can be measured, which gives access to the work of adhesion, that represents the total quantity of energy that was needed to break the interaction (in blue on Fig. 5A). For both adhesion force and work of adhesion, higher values indicate a stronger interaction between the cantilever and the sample. Finally, the rupture distance can be determined, which corresponds to the distance between the contact point (when the cantilever touches the surface) and the last adhesion peak on the curve (in red on Fig. 5A). This parameter is a function of the length of the molecules that are unfolded from the sample surface upon retraction. These three parameters allow describing the interactions recorded.

In a first step we examined the force curves obtained (Fig. 5B and C). When probing the interactions with cells grown with nitrate (Fig. 5B), the force curves all presented multiple retract adhesions on long distances, without a defined pattern. These force curves indicate the elongation of extended molecules from the cell wall interacting with Zn (Formosa et al., 2012; Feuillie et al., 2017). In the case of cells grown with ammonium, only 50.8% of the force curves presented adhesion peaks, meaning that the adhesion probability between Zn and cells in this condition is much lower. Then the curves that presented retract adhesions presented a small, single peak, close to the contact point. These first observations already show a clear tendency of Zn to interact with EPS but not with the cell wall. To quantify these differences, both the work of adhesion and the maximum adhesion force was measured (Fig. 5D and E). The adhesion forces recorded showed no significant differences between the two conditions: the average values are of 832.1 ± 1063.9 pN for cells grown with nitrate as the nitrogen source and of 764.9 ± 960.0 pN for cells grown with ammonium (Fig. 5E). Note the high heterogeneity of the measurements, which can be attributed to the natural heterogeneity of living cells and the potential differences in the size of the Zn particles used in the experiments. However, when measuring the work of adhesion, a significant difference can be observed between the two conditions, as the average value is of $14.2 \times 10^6 \pm 26.8 \times 10^6$ J for cells grown with nitrate and of $1.2 \times 10^6 \pm 2.0 \times 10^6$ J for cells grown with ammonium (Fig. 5D). Thus, while the force of the interaction is the same between the two conditions, which could mean that the same molecules are involved in the interaction, the amount of energy needed to break the interaction, and thus the number of molecules involved in the interactions is much larger in the case of cells grown with nitrate. Finally, regarding the rupture distances measured, they are of 5.2 ± 2.1 µm for cells grown with nitrate and of 0.4 ± 0.5 µm for cells grown with ammonium. These results mean that for cells grown with nitrate, upon retraction of the functionalized cantilever, long and most likely several molecules are unfolded from the surface, while this is not the case for cells grown with ammonium. To make sure that the interactions recorded correspond to interactions between Zn and cells, these experiments were then repeated in the same conditions (same applied force and contact time) with bare AFM tips. The results showed that in the case of cells grown with nitrate, 86.3% of the force curves obtained presented no adhesions, and that the adhesions recorded were of 40.5 ± 40.3 pN (Fig. S5A). For cells grown with ammonium, a similar % of force curves interact with the cantilever (54.0%) with a level of force significantly lower, of 365.3 ±412.8 pN (Fig. S5B). These control experiments thus prove that the interactions recorded with Zn particles are indeed due to the presence of the Zn particles on the

cantilevers. Altogether these results allow us to draw two conclusions: the first one is that Zn particles can interact with the cell wall of *P. kessleri* cells, but these interactions do not occur often (50.8% of adhesion) and involve a few molecules from the surface (single peaks and low distance ruptures). But this could explain the results obtained before regarding the biophysical properties of ammonium cells exposed to Zn (Fig. 3): while there is no strong attachment of the Zn particles on the surface of cells, the particles can still interact with it and could be a cause of the changes observed in terms of roughness and nanomechanical properties. The second conclusion is that the EPS produced by cells grown in nitrate conditions can interact with Zn particles *via* multiple bindings with long molecules. This results in the high work of adhesion recorded, and it highlights the key role probably played by the EPS in the remediation of Zn from the medium. Indeed, because of these strong adhesions, the Zn in the medium can penetrate into the EPS layer on the cells, from where it can then maybe diffuse into the cell and change its metabolism, and this way removing it from the culture medium.

While the role of EPS in the adsorption of pollutants is now a commonly accepted mechanism (Xiong et al., 2021; Nguyen et al., 2021), their role in the bioremediation of heavy metals is so far poorly documented. It is known that many microalgae species can be used to remediate heavy metals (Manikandan et al., 2022), however, in most studies, the role of EPS is not investigated. One reason for that can be because of a lack of technique allowing to prove their interactions with the metals. AFM is an ideal tool for that, but as far as we know, it has not been used in such studies except in one, where the role of EPS in the adsorption of Ag nanoparticles was demonstrated by imaging at high-resolution the EPS produced by cells after exposure to the nanoparticles (Pletikapić et al., 2012). Here, by functionalizing Zn particles at the edge of AFM cantilevers, it is possible to access their interactions with cells, and this way understand the molecular basis of the bioremediation mechanism.

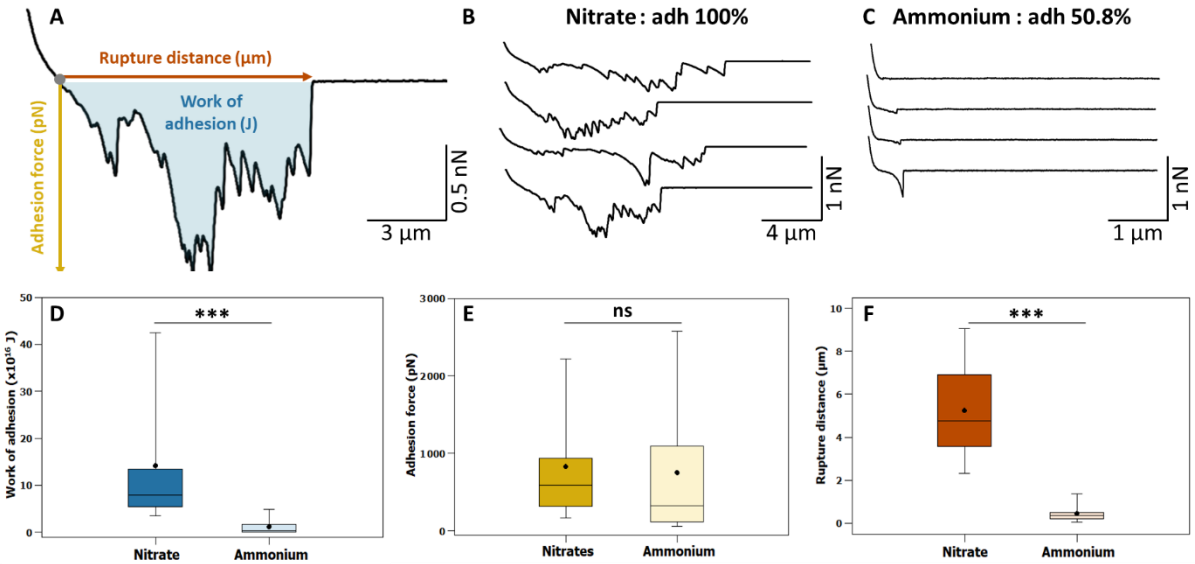

Fig. 5. Probing the interactions between Zn particles and P. kessleri cells. *A) scheme showing the different parameters that can be extracted from the force curves obtained. B) Force curves obtained in the case of cells grown with nitrate and C) in the case of cells grown with ammonium. D) Boxplot showing the distribution of the work of adhesion values obtained for cells in both nutritive conditions, E) of the adhesion force values, and F) of the rupture distances values*.

To further prove this point and confirm that the EPS produced by *P. kessleri* grown in the

534 presence of nitrate indeed absorb the zinc present in the medium, we next conducted dynamic

535 mechanical analysis (DMA) experiments using AFM. In this type of experiment, the idea is to

superpose low-amplitude sinusoidal oscillations to an initial indentation by a colloidal probe (Abidine

et al., 2013). Classic nanoindentation experiments, such as those previously performed (Fig. 2F and 3F), assume the material is purely elastic. However, since the EPS forms a soft gel-like structure around the cells, it is reasonable to assume that the viscous component is not negligible. Performing DMA experiments allows obtaining this information on the viscosity, by making it possible to decompose the elastic and the viscous parameters. In a first step, the shear storage (G') and the shear loss (G'') are determined, corresponding respectively to the elastic (solid) and to the viscous (liquid) behavior. These results presented in Fig. 6A show that in both conditions (cells grown in nitrate with or without Zn(II)), G' is higher than G'' at frequencies lower than 100 Hz, meaning that the EPS show a solid-like behavior in this regime. While for cells treated with Zn, this remains the case, for control cells (no Zn(II) exposure), G' and G'' values intersect at 100 Hz. This indicates that at these high frequencies, EPS are more viscous when cells were not exposed to Zn(II) than when they are. This is confirmed by looking at the loss tangent (ratio of G'' over G', Fig. 6B) that becomes superior to 1 at 100 Hz for control cells, while it is inferior to 1 for cells that have been exposed to Zn(II). Thus, these experiments show that the EPS do not behave the same way regarding their mechanical properties when cells have been exposed to Zn. In control conditions, the increase in the oscillating frequency causes the EPS to become viscous, while this is not the case for cells exposed to Zn. Most likely, this difference is caused by the presence of Zn particles within the EPS layer, thus

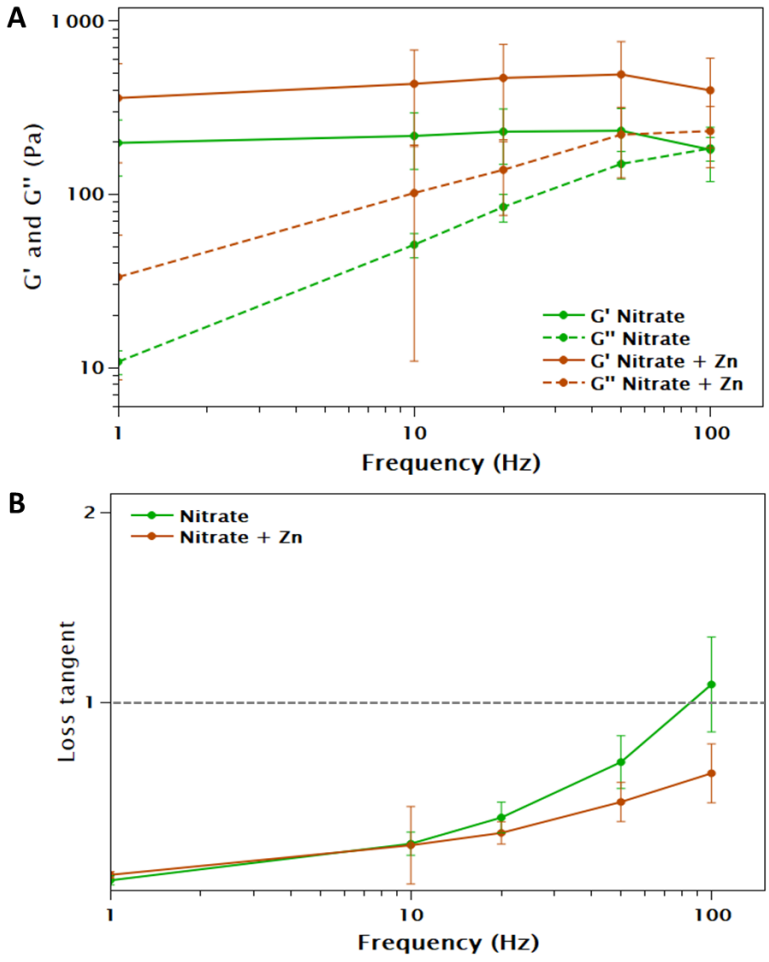

further proving our hypothesis that the Zn present in the medium is adsorbed by the EPS. Further experiments could be conducted to analyze the composition of extracted EPS before and after Zn(II) exposure, in order to understand if and how the heavy metal affects the EPS layer's composition.

Fig. 6. AFM dynamic mechanical analysis (DMA) of the EPS of P. kessleri cells grown with nitrate. *A) Viscoelastic modulus G' and G'' as a function of frequency for cells grown in the presence of nitrate, exposed (red lines) or not to Zn(II) (green lines). B) Loss tangent parameter (G''/G') for cells grown in the presence of nitrate, exposed (red line) or not to Zn(II) (green line).*

4. Conclusions

Microalgae are valuable for remediating pollutants, including heavy metals, from aquatic environments. To harness this potential for biotechnological applications, it is crucial to understand the conditions and mechanisms of their remediation abilities. This study used P. kessleri cells from the polluted Reconquista River, adapted to extremely polluted environments. We employed Raman spectroscopy and atomic force microscopy (AFM) to image these cells with different nitrogen sources, analyze their biophysical properties, and study their interactions with zinc particles. This original approach allowed to obtain the key following results:

- Cells grown with nitrate produce EPS, while those grown with ammonium do not
- AFM analysis showed that exposure to Zn(II) altered the surface roughness and nanomechanical properties of the cell wall and EPS.
- Raman spectroscopy indicated significant metabolic differences based on the nitrogen source, with Zn impacting cells grown with nitrate more than those grown with ammonium.
- AFM force spectroscopy results further demonstrated that Zn binds strongly to polymers in the EPS of nitrate-cultured cells, whereas interactions with ammonium-grown cells were weaker and less frequent.
- DMA experiments showed changes in the mechanical behavior of the EPS when cells have been exposed to Zn(II).

These results are summarized in Fig. 7. Altogether, they allow understanding the mechanism by which *P. kessleri* cells are able to remediate Zn, through its absorption in the EPS that cells produce when grown with nitrate as a nitrogen source. This study constitutes a unique contribution to the microalgae bioremediation of heavy metals by underscoring the pivotal role of ~~extracellular polymeric substances (~~EPS~~)~~ in the adsorption of Zn from the culture medium by the cells. It has also shed light on the significance of regulating the nitrogen source to induce the production of EPS in the cells. Consequently, this research offers crucial fundamental insights that could be applied in

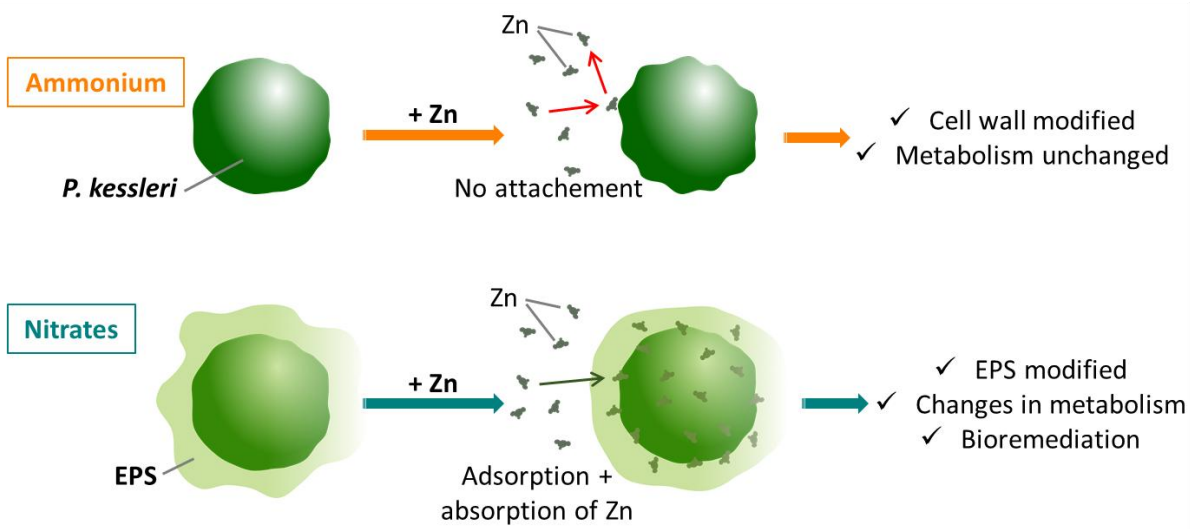

586 subsequent biotechnological endeavors aimed at decontaminating aquatic environments.

587 ***Fig. 7. Schematic representation of the Zn remediation mechanism by P. kessleri cells.***

588

589

Acknowledgements

C. F.-D. is a researcher at CNRS. The authors would like to express their gratitude to Alexia Pean for her contributions to this manuscript. In addition, we thank the PICTICEO facility dedicated to enzyme screening and discovery, and part of the Integrated Screening Platform of Toulouse (PICT, IBiSA) for providing access to the plasma generator. PICT-ICEO is a member of IBISBA-FR (https://doi.org/10. 15454/08BX-VJ91), the French node of the European research infrastructure, IBISBA (www.ibisba.eu). PICT-ICEO acknowledges funding support by the ANR grant Aladin (EQUIPEX+ grant number 15000882).

Statements & Declarations

The authors declare no competing financial interests

Funding

This work was supported by Consejo Nacional de Investigaciones Científicas y Técnicas (CONICET) (PIP 11220170100770CO); Universidad Nacional de San Martin that supported the travel expenses from Buenos Aires to the Toulouse Biotechnology Institute, and by an International Emerging Action (IEA) program of the CNRS (project ALGAREMEDIATION).

Data availability

The data will be available upon request.

Ethical approval

Not applicable

Consent to participate

All authors of this manuscript have provided their informed consent to participate in the study. They have agreed to contribute their expertise, data, and analysis to the research project. Final version was evaluated by all authors, who have read and approved the final manuscript.

Consent to publish

All authors of this manuscript have granted their consent for its publication. They acknowledge and agree to be held responsible for the content presented in the manuscript and affirm that it does not violate any copyright laws. Furthermore, they have reviewed and approved the final version of the manuscript before submission.

Competing interests

The authors have no relevant financial or non-financial interests to disclose.

References

Abidine, Y., Laurent, V.M., Michel, R., Duperray, A., Verdier, C., 2013. Microrheology of complex systems and living cells using AFM. Computer Methods in Biomechanics and Biomedical Engineering.

Afonso, V., Borges, R., Rodrigues, B., Barros, R., João Bebianno, M., Raposo, S., 2024. Are native microalgae consortia able to remove microplastics from wastewater effluents? Environmental Pollution 349, 123931. https://doi.org/10.1016/j.envpol.2024.123931

Areco, M.M., Haug, E., Curutchet, G., 2018. Studies on bioremediation of Zn and acid waters using Botryococcus braunii. Journal of Environmental Chemical Engineering 6, 3849–3859. https://doi.org/10.1016/j.jece.2018.05.041

Areco, M.M., Rojas, L., Noseda, D.G., Passucci, V., Rotella, N., Curutchet, G., 2022. Effect of nitrogen source and nickel concentration on green microalga Botryococcus braunii growth and its remediation potential. J Appl Phycol 34, 2941–2954. https://doi.org/10.1007/s10811-022-02847-3

Areco, M.M., Salomone, V.N., Afonso, M. dos S., 2021. Ulva lactuca: A bioindicator for anthropogenic contamination and its environmental remediation capacity. Marine Environmental Research 171, 105468. https://doi.org/10.1016/j.marenvres.2021.105468

Babiak, W., Krzemińska, I., 2021. Extracellular Polymeric Substances (EPS) as Microalgal Bioproducts: A Review of Factors Affecting EPS Synthesis and Application in Flocculation Processes. Energies 14, 4007. https://doi.org/10.3390/en14134007

Basílico, G., Ionno, V., Iglesias, G., Olivelli, M.S., de Cabo, L., 2022. Chapter 9 - Sediment pollution in aquatic environments of the metropolitan region of Buenos Aires, Argentina, in: Naeem, M., Aftab, T., Ali Ansari, A., Gill, S.S., Macovei, A. (Eds.), Hazardous and Trace Materials in Soil and Plants. Academic Press, pp. 97–110. https://doi.org/10.1016/B978-0-323-91632-5.00006-9

Bauenova, M.O., Sadvakasova, A.K., Mustapayeva, Z.O., Kokociński, M., Zayadan, B.K., Wojciechowicz, M.K., Balouch, H., Akmukhanova, N.R., Alwasel, S., Allakhverdiev, S.I., 2021. Potential of microalgae Parachlorella kessleri Bh-2 as bioremediation agent of heavy metals cadmium and chromium. Algal Research 59, 102463. https://doi.org/10.1016/j.algal.2021.102463

Beaussart, A., El-Kirat-Chatel, S., Sullan, R.M.A., Alsteens, D., Herman, P., Derclaye, S., Dufrêne, Y.F., 2014. Quantifying the forces guiding microbial cell adhesion using single-cell force spectroscopy. Nat. Protocols 9, 1049–1055. https://doi.org/10.1038/nprot.2014.066

Binnig, G., Quate, C.F., Gerber, C., 1986. Atomic Force Microscope. Physical Review Letters 56, 930–934.

Castañé, P.M., Loez, C.R., Olguín, H.F., Puig, A., Rovedatti, M.G., Topalián, M.L., Salibián, A., 1998. Caracterización y variación espacial de parámetros fisicoquímicos y del plancton en un río urbano contaminado, (río Reconquista, Argentina). Revista Internacional de Contaminación Ambiental 14, 69–77.

Ciempiel, W., Czemierska, M., Szymańska-Chargot, M., Zdunek, A., Wiącek, D., Jarosz-Wilkołazka, A., Krzemińska, I., 2022. Soluble Extracellular Polymeric Substances Produced by Parachlorella kessleri and Chlorella vulgaris: Biochemical Characterization and Assessment of Their Cadmium and Lead Sorption Abilities. Molecules 27, 7153. https://doi.org/10.3390/molecules27217153

Cordella, C.B.Y., Bertrand, D., 2014. SAISIR: A new general chemometric toolbox. TrAC Trends in Analytical Chemistry 54, 75–82. https://doi.org/10.1016/j.trac.2013.10.009

Cybulska, J., Halaj, M., Cepák, V., Lukavský, J., Capek, P., 2016. Nanostructure features of microalgae biopolymer. Starch - Stärke 68, 629–636. https://doi.org/10.1002/star.201500159

Dayana Priyadharshini, S., Suresh Babu, P., Manikandan, S., Subbaiya, R., Govarthanan, M., Karmegam, N., 2021. Phycoremediation of wastewater for pollutant removal: A green approach to environmental protection and long-term remediation. Environmental Pollution 290, 117989. https://doi.org/10.1016/j.envpol.2021.117989

Demir, I., Blockx, J., Dague, E., Guiraud, P., Thielemans, W., Muylaert, K., Formosa-Dague, C., 2020. Nanoscale Evidence Unravels Microalgae Flocculation Mechanism Induced by Chitosan. ACS Appl. Bio Mater. 3, 8446–8459. https://doi.org/10.1021/acsabm.0c00772

Demir-Yilmaz, I., Ftouhi, M.S., Balayssac, S., Guiraud, P., Coudret, C., Formosa-Dague, C., 2023a. Bubble functionalization in flotation process improve microalgae harvesting. Chemical Engineering Journal 452, 139349. https://doi.org/10.1016/j.cej.2022.139349

Demir-Yilmaz, I., Guiraud, P., Formosa-Dague, C., 2021. The contribution of Atomic Force Microscopy (AFM) in microalgae studies: A review. Algal Research 60, 102506. https://doi.org/10.1016/j.algal.2021.102506

Demir-Yilmaz, I., Novosel, N., Levak Zorinc, M., Mišić Radić, T., Ftouhi, M.S., Guiraud, P., Ivošević DeNardis, N., Formosa-Dague, C., 2023b. Investigation of the role of cell hydrophobicity and EPS production in the aggregation of the marine diatom Cylindrotheca closterium under hypo-saline conditions. Marine Environmental Research 188, 106020. https://doi.org/10.1016/j.marenvres.2023.106020

Demir-Yilmaz, I., Schiavone, M., Esvan, J., Guiraud, P., Formosa-Dague, C., 2023c. Combining AFM, XPS and chemical hydrolysis to understand the complexity and dynamics of C. vulgaris cell wall composition and architecture. Algal Research 72, 103102. https://doi.org/10.1016/j.algal.2023.103102

Demir-Yilmaz, I., Yakovenko, N., Roux, C., Guiraud, P., Collin, F., Coudret, C., ter Halle, A., Formosa-Dague, C., 2022. The role of microplastics in microalgae cells aggregation: A study at the molecular scale using atomic force microscopy. Science of The Total Environment 832, 155036. https://doi.org/10.1016/j.scitotenv.2022.155036

Dufrêne, Y.F., Ando, T., Garcia, R., Alsteens, D., Martinez-Martin, D., Engel, A., Gerber, C., Müller, D.J., 2017. Imaging modes of atomic force microscopy for application in molecular and cell biology. Nat Nanotechnol 12, 295–307. https://doi.org/10.1038/nnano.2017.45

Ferraro, G., Toranzo, R.M., Bagnato, C., Gómez Jousse, M., Areco, M.M., Bohé, A., Bagnarol, D., Pasquevich, D.M., Curutchet, G., 2021. Native *Desmodesmus* sp. and *Chlorella* sp. isolated from the Reconquista River display a different binding preference for Cu(II) and Zn(II). Journal of Environmental Management 293, 112835. https://doi.org/10.1016/j.jenvman.2021.112835

Feuillie, C., Formosa-Dague, C., Hays, L.M.C., Vervaeck, O., Derclaye, S., Brennan, M.P., Foster, T.J., Geoghegan, J.A., Dufrêne, Y.F., 2017. Molecular interactions and inhibition of the staphylococcal biofilm-forming protein SdrC. Proc Natl Acad Sci U S A 114, 3738–3743. https://doi.org/10.1073/pnas.1616805114

Formosa, C., Grare, M., Jauvert, E., Coutable, A., Regnouf-de-Vains, J.B., Mourer, M., Duval, R.E., Dague, E., 2012. Nanoscale analysis of the effects of antibiotics and CX1 on a Pseudomonas aeruginosa multidrug-resistant strain. Sci. Rep. 2. https://doi.org/10.1038/srep00575

Formosa-Dague, C., Gernigon, V., Castelain, M., Daboussi, F., Guiraud, P., 2018. Towards a better understanding of the flocculation/flotation mechanism of the marine microalgae Phaeodactylum tricornutum under increased pH using atomic force microscopy. Algal Research 33, 369–378. https://doi.org/10.1016/j.algal.2018.06.010

Grimolizzi, M.C., 2019. Aislamiento y caracterización de bacterias autóctonas, con potencial en biolixiviación de sedimentos del Río Reconquista. Universidad Nacional de San Martin, Argentina.

Gupta, P., Diwan, B., 2017. Bacterial Exopolysaccharide mediated heavy metal removal: A Review on biosynthesis, mechanism and remediation strategies. Biotechnology Reports 13, 58–71. https://doi.org/10.1016/j.btre.2016.12.006

Hasani Zadeh, P., Fermoso, F.G., Collins, G., Serrano, A., Mills, S., Abram, F., 2023. Impacts of metal stress on extracellular microbial products, and potential for selective metal recovery. Ecotoxicology and Environmental Safety 252, 114604. https://doi.org/10.1016/j.ecoenv.2023.114604

He, J., Chen, J.P., 2014. A comprehensive review on biosorption of heavy metals by algal biomass: Materials, performances, chemistry, and modeling simulation tools. Bioresource Technology, Special Issue on Biosorption 160, 67–78. https://doi.org/10.1016/j.biortech.2014.01.068

He, S., Fang, S., Xie, W., Zhang, P., Li, Z., Zhou, D., Zhang, Z., Guo, J., Du, C., Du, J., Wang, D., 2018. Assessment of physiological responses and growth phases of different microalgae under environmental changes by Raman spectroscopy with chemometrics. Spectrochimica Acta Part A: Molecular and Biomolecular Spectroscopy 204, 287–294. https://doi.org/10.1016/j.saa.2018.06.060

Hertz, H., 1881. Ueber die beruhrung fester elastischer korper. Journal fur die reine und angewandte mathematik 156–171.

Hutter, J.L., Bechhoefer, J., 1993. Calibration of atomic-force microscope tips. Review of Scientific Instruments 64, 1868–1873.

Ivošević DeNardis, N., Pečar Ilić, J., Ružić, I., Novosel, N., Mišić Radić, T., Weber, A., Kasum, D., Pavlinska, Z., Balogh, R.K., Hajdu, B., Marček Chorvátová, A., Gyurcsik, B., 2019. Algal cell response to laboratory-induced cadmium stress: a multimethod approach. Eur Biophys J 48, 231–248. https://doi.org/10.1007/s00249-019-01347-6

Kakade, A., Salama, E.-S., Han, H., Zheng, Y., Kulshrestha, S., Jalalah, M., Harraz, F.A., Alsareii, S.A., Li, X., 2021. World eutrophic pollution of lake and river: Biotreatment potential and future perspectives. Environmental Technology & Innovation 23, 101604. https://doi.org/10.1016/j.eti.2021.101604

Kruskal, W.H., Wallis, W.A., 1952. Use of Ranks in One-Criterion Variance Analysis. Journal of the American Statistical Association 47, 583–621. https://doi.org/10.2307/2280779

Li, C., Yu, Y., Fang, A., Feng, D., Du, M., Tang, A., Chen, S., Li, A., 2022. Insight into biosorption of heavy metals by extracellular polymer substances and the improvement of the efficacy: a review. Letters in Applied Microbiology 75, 1064–1073. https://doi.org/10.1111/lam.13563

Li, H., Meng, F., 2023. Efficiency, mechanism, influencing factors, and integrated technology of biodegradation for aromatic compounds by microalgae: A review. Environmental Pollution 335, 122248. https://doi.org/10.1016/j.envpol.2023.122248

Li, X., Sha, J., Chu, B., Wei, Y., Huang, W., Zhou, H., Xu, N., He, Y., 2019. Quantitative visualization of intracellular lipids concentration in a microalgae cell based on Raman micro-spectroscopy coupled with chemometrics. Sensors and Actuators B: Chemical 292, 7–15. https://doi.org/10.1016/j.snb.2019.04.048

Lieutaud, C., Assaf, A., Gonçalves, O., Wielgosz-Collin, G., Thouand, G., 2019. Fast non-invasive monitoring of microalgal physiological stage in photobioreactors through Raman spectroscopy. Algal Research 42, 101595. https://doi.org/10.1016/j.algal.2019.101595

Lupi, F.M., Fernandes, H.M.L., Tomé, M.M., Sá-Correia, I., Novais, J.M., 1994. Influence of nitrogen source and photoperiod on exopolysaccharide synthesis by the microalga Botryococcus braunii UC 58. Enzyme and Microbial Technology 16, 546–550. https://doi.org/10.1016/0141-0229(94)90116-3

Lv, J., Wang, X., Feng, J., Liu, Q., Nan, F., Jiao, X., Xie, S., 2019. Comparison of growth characteristics and nitrogen removal capacity of five species of green algae. J Appl Phycol 31, 409–421. https://doi.org/10.1007/s10811-018-1542-y

Manikandan, A., Suresh Babu, P., Shyamalagowri, S., Kamaraj, M., Muthukumaran, P., Aravind, J., 2022. Emerging role of microalgae in heavy metal bioremediation. Journal of Basic Microbiology 62, 330–347. https://doi.org/10.1002/jobm.202100363

Nguyen, H.T., Yoon, Y., Ngo, H.H., Jang, A., 2021. The application of microalgae in removing organic micropollutants in wastewater. Critical Reviews in Environmental Science and Technology 51, 1187–1220. https://doi.org/10.1080/10643389.2020.1753633

O'Rourke, R., Gaffney, M., Murphy, R., 2015. The effects of Parachlorella kessleri cultivation on brewery wastewater. Water Science and Technology 73, 1401–1408. https://doi.org/10.2166/wst.2015.618

778 Pillet, F., Dague, E., Pečar Ilić, J., Ružić, I., Rols, M.-P., Ivošević DeNardis, N., 2019. Changes in
779 nanomechanical properties and adhesion dynamics of algal cells during their growth.
780 Bioelectrochemistry 127, 154–162. https://doi.org/voelcker
781 Pletikapić, G., Žutić, V., Vrček, I.V., Svetličić, V., 2012. Atomic force microscopy characterization of
782 silver nanoparticles interactions with marine diatom cells and extracellular polymeric
783 substance. Journal of Molecular Recognition 25, 309–317. https://doi.org/10.1002/jmr.2177
784 Rude, K., Yothers, C., Barzee, T.J., Kutney, S., Zhang, R., Franz, A., 2022. Growth potential of
785 microalgae on ammonia-rich anaerobic digester effluent for wastewater remediation. Algal
786 Research 62, 102613. https://doi.org/10.1016/j.algal.2021.102613
787 Sasaki, M., Takagi, A., Ota, S., Kawano, S., Sasaki, D., Asayama, M., 2020. Coproduction of lipids and
788 extracellular polysaccharides from the novel green alga Parachlorella sp. BX1.5 depending on
789 cultivation conditions. Biotechnology Reports 25, e00392.
790 https://doi.org/10.1016/j.btre.2019.e00392
791 Satya, A.D.M., Cheah, W.Y., Yazdi, S.K., Cheng, Y.-S., Khoo, K.S., Vo, D.-V.N., Bui, X.D., Vithanage, M.,
792 Show, P.L., 2023. Progress on microalgae cultivation in wastewater for bioremediation and
793 circular bioeconomy. Environmental Research 218, 114948.
794 https://doi.org/10.1016/j.envres.2022.114948
795 Sendra, M., Moreno-Garrido, I., Yeste, M.P., Gatica, J.M., Blasco, J., 2017. Toxicity of TiO2, in
796 nanoparticle or bulk form to freshwater and marine microalgae under visible light and UV-A
797 radiation. Environmental Pollution 227, 39–48. https://doi.org/10.1016/j.envpol.2017.04.053
798 Spain, O., Plöhn, M., Funk, C., 2021. The cell wall of green microalgae and its role in heavy metal
799 removal. Physiologia Plantarum 173, 526–535. https://doi.org/10.1111/ppl.13405
800 Sreenikethanam, A., Raj, S., J, R.B., Gugulothu, P., Bajhaiya, A.K., 2022. Genetic Engineering of
801 Microalgae for Secondary Metabolite Production: Recent Developments, Challenges, and
802 Future Prospects. Front. Bioeng. Biotechnol. 10. https://doi.org/10.3389/fbioe.2022.836056
803 Tripathi, S., Kairamkonda, M., Gupta, P., Poluri, K.M., 2023. Dissecting the molecular mechanisms of
804 producing biofuel and value-added products by cadmium tolerant microalgae as sustainable
805 biorefinery approach. Chemical Engineering Journal 454, 140068.
806 https://doi.org/10.1016/j.cej.2022.140068
807 Tripathi, S., Poluri, K.M., 2021. Heavy metal detoxification mechanisms by microalgae: Insights from
808 transcriptomics analysis. Environmental Pollution 285, 117443.
809 https://doi.org/10.1016/j.envpol.2021.117443
810 Tufo, A.E., Porzionato, N.F., Curutchet, G., 2018. Effects of pollution and bioleaching process on the
811 mineral composition and texture of contaminated sediments of the Reconquista River,
812 Argentina. Environ Sci Pollut Res 25, 21368–21384. https://doi.org/10.1007/s11356-017-
813 0484-2
814 Vergnes, J.-B., Gernigon, V., Guiraud, P., Formosa-Dague, C., 2019. Bicarbonate concentration
815 induces production of exopolysaccharides by Arthrospira platensis that mediate bio-
816 flocculation and enhance flotation harvesting efficiency. ACS Sustainable Chem. Eng.
817 https://doi.org/10.1021/acssuschemeng.9b01591
818 Volesky, B., 2007. Biosorption and me. Water Research 41, 4017–4029.
819 https://doi.org/10.1016/j.watres.2007.05.062
820 Wang, B.-B., Liu, X.-T., Chen, J.-M., Peng, D.-C., He, F., 2018. Composition and functional group
821 characterization of extracellular polymeric substances (EPS) in activated sludge: the impacts
822 of polymerization degree of proteinaceous substrates. Water Research 129, 133–142.
823 https://doi.org/10.1016/j.watres.2017.11.008
824 Wang, M., Kuo-Dahab, W.C., Dolan, S., Park, C., 2014. Kinetics of nutrient removal and expression of
825 extracellular polymeric substances of the microalgae, *Chlorella* sp. and *Micractinium* sp., in
826 wastewater treatment. Bioresource Technology 154, 131–137.
827 https://doi.org/10.1016/j.biortech.2013.12.047
828 Wieser, W., Assaf, A.A., Le Gouic, B., Dechandol, E., Herve, L., Louineau, T., Dib, O.H., Gonçalves, O.,
829 Titica, M., Couzinet-Mossion, A., Wielgosz-Collin, G., Bittel, M., Thouand, G., 2023.

Development and Application of an Automated Raman Sensor for Bioprocess Monitoring: From the Laboratory to an Algae Production Platform. Sensors 23, 9746. https://doi.org/10.3390/s23249746

Xiao, R., Zheng, Y., 2016. Overview of microalgal extracellular polymeric substances (EPS) and their applications. Biotechnology Advances 34, 1225–1244. https://doi.org/10.1016/j.biotechadv.2016.08.004

Xiong, Q., Hu, L.-X., Liu, Y.-S., Zhao, J.-L., He, L.-Y., Ying, G.-G., 2021. Microalgae-based technology for antibiotics removal: From mechanisms to application of innovational hybrid systems. Environment International 155, 106594. https://doi.org/10.1016/j.envint.2021.106594

Yap, B.H.J., Crawford, S.A., Dagastine, R.R., Scales, P.J., Martin, G.J.O., 2016. Nitrogen deprivation of microalgae: effect on cell size, cell wall thickness, cell strength, and resistance to mechanical disruption. Journal of Industrial Microbiology and Biotechnology 43, 1671–1680. https://doi.org/10.1007/s10295-016-1848-1

Ye, T., Yang, A., Wang, Y., Song, N., Wang, P., Xu, H., 2022. Changes of the physicochemical properties of extracellular polymeric substances (EPS) from *Microcystis aeruginosa* in response to microplastics. Environmental Pollution 315, 120354. https://doi.org/10.1016/j.envpol.2022.120354

Zhang, P., Li, Z., Lu, L., Xiao, Y., Liu, J., Guo, J., Fang, F., 2017. Effects of stepwise nitrogen depletion on carotenoid content, fluorescence parameters and the cellular stoichiometry of *Chlorella vulgaris*. Spectrochimica Acta Part A: Molecular and Biomolecular Spectroscopy 181, 30–38. https://doi.org/10.1016/j.saa.2017.03.022